Analytical solitary-wave solutions of the generalized nonautonomous cubic-quintic nonlinear Schrödinger equation with different external potentials

Jun-Rong He and Hua-Mei Li[*]

Department of Physics, Zhejiang Normal University, Jinhua, Zhejiang 321004, People's Republic of China
(Received 14 October 2010; revised manuscript received 4 January 2011; published 28 June 2011)

A large family of analytical solitary wave solutions to the generalized nonautonomous cubic-quintic nonlinear Schrödinger equation with time- and space-dependent distributed coefficients and external potentials are obtained by using a similarity transformation technique. We use the cubic nonlinearity as an independent parameter function, where a simple procedure is established to obtain different classes of potentials and solutions. The solutions exist under certain conditions and impose constraints on the coefficients depicting dispersion, cubic and quintic nonlinearities, and gain (or loss). We investigate the space-quadratic potential, optical lattice potential, flying bird potential, and potential barrier (well). Some interesting periodic solitary wave solutions corresponding to these potentials are then studied. Also, properties of a few solutions and physical applications of interest to the field are discussed. Finally, the stability of the solitary wave solutions under slight disturbance of the constraint conditions and initial perturbation of white noise is discussed numerically; the results reveal that the solitary waves can propagate in a stable way under slight disturbance of the constraint conditions and the initial perturbation of white noise.

I. INTRODUCTION

The nonlinear Schrödinger (NLS) equation is one of the most important nonlinear models of modern science. It appears in many branches of physics, including plasma physics [1], nonlinear optics [2], and Bose-Einstein condensates (BECs) [3]. Theoretically, there have been many methods for solving it, such as the inverse scattering transform (IST), the Darboux-Bäcklund transform (DBT), the variational approach, and the symmetrical reduction technique. In general, DBT and IST require that the governing equation has to pass the Painlevé PDE test. The best-known solutions of the NLS equation are those for solitary waves or solitons. Properties of these solutions are well studied in the literature [4,5].

It is known that the classical soliton concept emerges from the autonomous systems who have constant distributed coefficients. Generally, these systems have no significant effects on the control of soliton's shape. A general situation is one in which a system receives some form of external time-dependent or space-dependent force, namely a nonautonomous system. Such situations support temporal or spatial solitons, soliton lasers, and ultrafast soliton switches for experiments [6,7]. Recently, a nonautonomous system with distributed coefficients has attracted a lot of attention because of its interesting features and potential applications [8–11]. More generally, nonautonomous systems with time- and space-dependent distributed coefficients also have very interesting properties but have been the subject of relatively fewer studies.

On the other hand, when the intensity of the optical pulse propagating inside nonlinear medium exceeds a certain value or the two- and three-body interactions in BECs are considered, the governing equation should still include the cubic and quintic (CQ) nonlinearities. Thus, in nonautonomous systems, a generalized nonautonomous NLS equation with the CQ nonlinearities as well as the gain or loss is presented. Recently,

the CQ model has received much attention [12] due to intensive research in nonlinear optics [13], not only the one-dimensional model [14,15] but also the corresponding two-dimensional vortex solitons in nonlinear media [16,17].

Based on the above discussions, in this paper we consider a generalized nonautonomous cubic-quintic nonlinear Schrödinger (CQNLS) equation with an external potentials describing soliton management in nonlinear optics [18]. We provide the analytical solutions of it, and most of them differ from the conventional solutions in many aspects because both amplitudes and speeds of the soliton solutions vary with time and space. In the one-dimensional case, the generalized nonautonomous CQNLS equation can be given by the following dimensionless form:

$$
\begin{aligned}
i\frac{\partial \psi}{\partial t} + f(x,t)\frac{\partial^2 \psi}{\partial x^2} + g(x,t)|\psi|^2\psi + G(x,t)|\psi|^4\psi \\
+ V(x,t)\psi + i\gamma(x,t)\psi = 0,
\end{aligned}
\tag{1}
$$

where $\psi(x,t)$ is the complex envelope of the electric field, x is the transverse variable, and t is the longitudinal variable. In the case of temporal solitons in optical fibers, t and x represent the propagation distance and the retarded time, respectively. $f(x,t)$ is the dispersion management parameter related to the linear refractive index n_0 and then $g(x,t)$ and $G(x,t)$ are related to the cubic nonlinearity coefficient n_2 and the quintic nonlinearity coefficient n_4, respectively. $V(x,t)$ is the external potential and $\gamma(x,t)$ is the gain or loss function. The linear refractive index n_0 is usually nonuniform distribution in the longitudinal direction (propagation direction) in nonlinear media, which leads the dispersion coefficient varies with the longitudinal variable. If the transverse direction of the nonlinear medium is also inhomogeneous, the linear refractive index n_0 can also be function of transverse variable, that is, $n_0 = n_0(x,t)$ in our model. Then the corresponding dispersion coefficient and other management coefficients can be function both in transverse and longitudinal directions. Recently, a novel type of Bloch cavity solitons existing in nonlinear

_____
[*]lihuamei@zjnu.cn

resonators with the refractive index modulated in both transverse and longitudinal directions have been presented [19]. This may provide a physical motivation for the purpose of our work.

It is noted that Eq. (1) can also describe the dynamics of matter-wave solitons in BECs where the soliton management can be realized by adjusting the related control parameters via the technique of Feshbach resonance [20,21]. In this case, t and x represent the time and spatial coordinate, respectively. If $f(x,t) = 1, \gamma(x,t) = 0$, Eq. (1) can be reduced into the CQNLS equation with external potential, which has been studied in Refs. [22,23]. When $f(x,t) \neq 1, \gamma(x,t) \neq 0$, Eq. (1) cannot pass the Painlevé PDE test, and the DBT or IST method fail to solve it. To resolve this problem, we give a similarity transformation technique to deal with Eq. (1) in this paper.

During the past several years, there has been a great deal of attention focused on the similarity transformation technique [22,24]. This method has been applied successfully to the NLS equations with varied coefficients. Recent studies in Ref. [25] are the most typical ones among them. More recently, in the work by He *et al.* [26], the generalized nonautonomous cubic NLS equation [Eq. (1) when $G(x,t) = 0$] is dealt with by using the Painlevé analysis, and the soliton solutions under integrability conditions is found when the dissipation or gain is vanishing ($\gamma = 0$). They obtained that the external potential is the quadratic coordinate term [$V(x,t) = V_0(t) + V_1(t)x + V_2(t)x^2$], while the coefficients depicting dispersion, CQ nonlinearities, and gain (or loss) can be only functions of time. Until now, no attempts had been made to find nontrivial laws of soliton adaptation in external potentials when management parameters and the confining potential in Eq. (1) complement each other. On the basis of this motivation, we extend the similarity transformation method to solve our model (1). The results allow one to obtain exact solutions under certain conditions and impose constraint conditions on the management parameters depicting dispersion, CQ nonlinearities, and gain (or loss). It should be pointed out that with the similarity transformation method used in this paper, a more general expression of the external potential containing the case in Ref. [26] can be obtained although we have the quintic nonlinearity item. That is, we extend the situations in Ref. [26] and obtain more general results without using any Painlevé analysis. This may provide the way to design external potential in nonlinear systems and to make soliton control more possible.

Equation (1) can be viewed as the evolution equation $\psi_t = \frac{\delta \mathcal{H}}{\delta(i\psi^*)}$, where $\mathcal{H}$ is the Hamiltonian function

$$\mathcal{H} = -\int_{-\infty}^{\infty} [\psi^* f(x,t)\triangle\psi + g(x,t)|\psi|^4 + G(x,t)|\psi|^6 \\ + V(x,t)|\psi|^2 + i\gamma(x,t)|\psi|^2]dx.$$

Generally speaking, the Hamiltonian $\mathcal{H}$ in our model (1) is not conserved. It will be seen that this situation would be changed by employing a similarity transformation technique, and the Hamiltonian $\mathcal{H}$ can be conserved under some cases.

The paper is organized as follows: In Sec. II, we provide the similarity transformation to change the generalized nonautonomous CQNLS equation to an autonomous one, which is

easier to solve. At the same time, the required integrability conditions, including explicit expression of external potential for exact solutions, are found. Solutions of the autonomous CQNLS equation are given. In Sec. III, we present two classes of solutions. First, in the absence of an external potential, Eq. (1) can have standard and periodic solitary wave solutions. Second, four types of periodic potentials are discussed, including the space-quadratic (SQ) potential [22,24,27,28], the optical lattice (OL) potential [29], the flying bird (FB) potential [23], and the potential barrier (well) [30]. It is shown that Eq. (1) can reduce to the generalized nonautonomous CQNLS equation with time-dependent coefficients under SQ potential and the Hamiltonian $\mathcal{H}$ can conserve in this equation when some parameters are chose properly. Exact solitary wave solutions corresponding to different potentials are presented under certain conditions. Representative properties of some solutions are studied, such as width, wave center position, and amplitude. Finally, the stability of the solitary waves under slight disturbance of the constraint conditions and initial perturbation of white noise is discussed numerically; the results reveal that the solitary waves can propagate in a stable way under slight disturbance of the constraint conditions and the initial perturbation of white noise. In Sec. IV, the main results of the paper are summarized.

II. GENERAL SIMILARITY TRANSFORMATION

In this work, we use a similarity transformation to construct explicit solutions for Eq. (1), as explained below.

The idea is to write the solution of (1) as

$$\psi(x,t) = \rho(x,t)\Phi(X(x,t),T(t))e^{i\phi(x,t)} \tag{2}$$

and then reduce (1) to the autonomous CQNLS equation

$$i\frac{\partial}{\partial T}\Phi + \frac{1}{2}\frac{\partial^2}{\partial X^2}\Phi + g_0|\Phi|^2\Phi + G_0|\Phi|^4\Phi = 0, \tag{3}$$

where $\rho(x,t), \phi(x,t), X(x,t), T(t)$ are real functions to be determined, $\Phi(X,T)$ is the solution of Eq. (3), and g_0 and G_0 are real constants.

We take $X(x,t) = \int_0^\xi F[\xi'(x,t)]d\xi'$ with $\xi(x,t) = \alpha(t)x$, where $F(\xi)$ is a key function to be elected and $\alpha(t)$ is an positive definite function of time. For this choice, we can determine the width of some solutions in the form $1/\alpha(t)$, which will be discussed in detail below. In order to look for exact solutions of (1), we suppose that the cubic nonlinearity is given of the form

$$g(x,t) = \alpha(t)F(\xi). \tag{4}$$

This choice is appropriate and necessary because it will lead external potential and other coefficients to be expressed well.

Substituting Eq. (2) into Eq. (1) by considering the ansatz of $X(x,t)$ and $g(x,t)$, and requiring that $\Phi(X,T)$ to satisfy Eq. (3), we have a system of partial differential equations (PDEs). By solving these PDEs, one finds the following solutions:

$$\rho(x,t) = \sqrt{\frac{a}{\alpha F(\xi)}}, \tag{5a}$$

$$T(t) = g_0^{-1}\int_0^t a(t')\,dt' + T_0, \tag{5b}$$

$$\phi(x,t) = -g_0 a^{-1} \alpha \alpha_t \int_0^x F^2(\xi) x' \, dx', \qquad (5c)$$

where $a = a(t)$ is arbitrary function of time and T_0 is arbitrary real constant. Note that the integral function of time in Eq. (5c) is chose to be zero. It should be pointed out that $g(x,t), G(x,t), f(x,t)$, and $\gamma(x,t)$ are not arbitrary but have the relationship:

$$\gamma = \frac{\alpha_t}{\alpha} \left(\frac{g_x}{g} x + 1 \right) - \frac{g_0^2 f_t G}{G_0} - \frac{g_t}{g} \qquad (6)$$

with

$$f = \frac{a}{2 g_0 \alpha^2 F(\xi)^2}, \quad G = \frac{G_0 \alpha^2 F(\xi)^2}{g_0 a}, \qquad (7)$$

where $g_0 \neq 0, G_0 \neq 0$. Therefore, as long as one chooses the parameters $a(t), \alpha(t)$, $F(\xi)$, one obtains the expressions of the coefficients in Eq. (1).

Now the expression of the potential is given by

$$V(x,t) = q_1(\xi,t) x^2 + \int_0^x [q_2(\xi,t) x' - q_3(\xi,t) x'^2] dx' + q_4(\xi,t) \qquad (8)$$

with

$$q_1(\xi,t) = \frac{g_0 \alpha_t^2 F^2(\xi)}{2a},$$

$$q_2(\xi,t) = \frac{g_0 F^2(\xi) (\alpha \alpha_t a_t - a \alpha \alpha_{tt} - a \alpha_t^2)}{a^2},$$

$$q_3(\xi,t) = \frac{2 g_0 F(\xi) F'(\xi) \alpha \alpha_t^2}{a},$$

$$q_4(\xi,t) = \frac{a[2 F(\xi) F''(\xi) - 3 F'^2(\xi)]}{8 g_0 F^4(\xi)},$$

where $F'(\xi) = dF/d\xi, F''(\xi) = d^2 F/d\xi^2$. From the above equations one can see that the external potential $V(x,t)$ is also not arbitrary but related to $g(x,t), G(x,t), f(x,t)$, and $\gamma(x,t)$ via the parameters $a(t)$, $\alpha(t)$, and $F(\xi)$. Thus, Eqs. (6)–(8) can be understood as integrability conditions on Eq. (1) for exact solutions by the method used in the paper.

Expression (8) can give rise to many sets of external potentials and CQ nonlinearities by the choices of independent parameters $\alpha(t), F(\xi)$. Note that we can also obtain the potential in Ref. [26]. For example, we can obtain $V(x,t) = V_0(t)$ by choosing $\alpha(t) = \alpha_0$, and $F(\xi)$ satisfy $2 F(\xi) F''(\xi) - 3 F'^2(\xi) - 8 g_0 F^4(\xi) = 0$, with $V_0(t) = a$; $V(x,t) = V_1(t) x$ by choosing $\alpha(t) = 1$, and $F(\xi)$ satisfy $2 F(\xi) F''(\xi) - 3 F'^2(\xi) - 8 g_0 \xi F^4(\xi) = 0$ (in this case, $\xi = x$), with $V_1(t) = a$; $V(x,t) = V_2(t) x^2$ by choosing $F(\xi) = F_0$, with $V_2(t) = \theta^2(t)$ [see Eq. (15) below]. Besides, some other interesting external potentials can be obtained, such as the OL potential, the FB potential, and the potential barrier (well), which will be discussed in detail below. To summarize in one sentence, the most important feature that distinguishes our situation from that reported in the literature [26] is that a more general expression (8) is obtained, which not only contains the previous case but also generates some other interesting specific external potentials.

It has been proven that exact solutions of Eq. (3) can exist under the solvable condition $G_0 = -\beta_0 g_0^2$ [31], where β_0 is

the arbitrary real constant. In this case, Eq. (3) has brightlike and darklike soliton solutions, depending on the sign of g_0 that controls the cubic nonlinearity in a specific system. If $g_0 > 0$, the brightlike soliton solution of Eq. (3) can be written in the form

$$\Phi_B(X,T) = \frac{M}{\sqrt{g_0}} \frac{\exp[iwX + i(\sigma - w^2/2)T]}{\sqrt{1 + N \cosh[p(X - wT)]}}, \qquad (9)$$

where $\sigma = \frac{3}{16\beta_0}(1 - N^2), M = 2\sqrt{\sigma}, p = 2\sqrt{2\sigma}$, and N is real number. Here w, p, and M are relative to the group velocity, the pulse width, and the amplitude, respectively.

When $g_0 < 0$, the darklike soliton solution can be given by

$$\Phi_D(X,T) = \frac{M}{\sqrt{-g_0}} \frac{\sinh[p(X - wT)]}{\sqrt{1 + N \sinh^2[p(X - wT)]}}$$
$$\times \exp[iwX - i(\sigma + w^2/2)T], \qquad (10)$$

where $\sigma = \frac{(3N-1)p^2}{2}$, $M = \sqrt{(3N - 2)p^2 N}$, and $p = \sqrt{\frac{3(N-1)}{2\beta_0(3N-2)^2}}$. It is clear that, to ensure the parameters to be real, we must have $N > 1$.

With the solutions of the autonomous CQNLS equation (3) given above, one can obtain the exact solitary wave solutions of Eq. (1). As can be seen, Eq. (9) leads to the wave function that solves Eq. (1) in a bright solitary wave solution

$$\psi_B(x,t) = \rho(x,t) \Phi_B(X,T) e^{i\phi(x,t)} \quad (g_0 > 0), \qquad (11)$$

and Eq. (10) leads to a dark solitary wave solution

$$\psi_D(x,t) = \rho(x,t) \Phi_D(X,T) e^{i\phi(x,t)} \quad (g_0 < 0). \qquad (12)$$

In our solutions, as long as one chooses the forms of the arbitrary functions $a(t), \alpha(t)$, and $F(\xi)$, one obtains the exact solitary wave solutions to the generalized nonautonomous CQNLS equation (1).

As can be seen from Eqs. (2), (4), and (5), when $\int_{-\infty}^{\infty} |\psi|^2 dx = $ const, we must have

$$\frac{a(t)}{g(x,t)^2} = \text{const}, \qquad (13)$$

that is, the dispersion $f(x,t)$ is a constant. This requires that the function $F(\xi)$ is time dependent or a constant. In this case, $\rho(x,t)$ is time dependent and the phase $\phi(x,t)$ has the quadratic nature with respect to the coordinate x. Therefore, the Hamiltonian $\mathcal{H}$ can be conserved under Eq. (13). This phenomena will be clearly shown in Sec. III.

It is worth pointing out that we can obtain the moving solutions and directly controlling them by changing Eq. (1) to the nonlinear Eq. (3), which is a partial differential equation possessing periodic solutions even without the time and space modulations of the potentials and coefficients.

III. SOME CHARACTERISTIC ANALYTICAL SOLITARY WAVE SOLUTIONS

In this section, we cite examples to illustrate some features of our exact analytic solutions (11) and (12) by considering the cubic nonlinearity distribution of special forms. For this, some interesting and useful external potentials are given with the choices of $a(t)$, $\alpha(t)$, and $F(\xi)$, and the corresponding

management coefficients are presented. We have four cases of the external potential according to $\alpha(t)$ or $F(\xi)$:

(i) $\alpha(t) = \alpha_0, F(\xi) = F_0$, leading *vanishing potential*.

(ii) $F(\xi) = F_0$, leading *SQ potential*.

(iii) $\alpha(t) = \alpha_0$, leading *OL potential*.

(iv) $\alpha(t)$ and $F(\xi)$ are general functions, leading *FB potential* and *potential barrier* (well).

Interest for research on these external potentials has never stopped and has attracted wide attention [22,24,27,30]. We will discuss these cases in detail below. Then, some interesting explicit analytical solitary wave solutions are generated, including decaying solitary waves, snakelike solitary waves, and solitary waves in an OL potential. Representative properties of some solutions are studied, such as width, wave center position, and amplitude, and most of them can be controlled by some parameters management [such as $a(t)$ and $\alpha(t)$]. This situation will be apparently seen below by using their exact expressions. Here we note that we will use

$$\alpha(t) = 1 + \epsilon \cos(\omega_0 t), \quad a(t) = 1 + a_0 \cos(\omega_1 t), \quad (14)$$

when they are arbitrary functions of time where required, with $\epsilon, a_0 \in (-1,1)$, $\omega_0, \omega_1 \in \mathbb{R}$. Also note that we will always take the parameters in our solutions to be $N = 0.5, g_0 = 1$ for brightlike types, and $N = 2, g_0 = -1$ for darklike types, and $F_0 = \omega_0 = \omega_1 = 1, T_0 = 0$ for both cases.

A. Vanishing potential [$\alpha(t) = \alpha_0, F(\xi) = F_0$]

First, we study the evolution of Eq. (1) in the absence of an external potential, namely $V(x,t) = 0$. In this case $\alpha(t) = \alpha_0$, $F(\xi) = F_0$, which yields constant phase in Eq. (5c). The coefficients in Eq. (1) are dependent on the time-dependent parameter a except for cubic nonlinearity $g(x,t)$. With this we can find that $\rho(x,t) = \sqrt{a/F_0\alpha_0}$ is time dependent and $X(x,t) = F_0\alpha_0 x$ is space dependent. We pay close attention to the following two cases according to $a(t)$.

(i) *Standard solitary waves.* When $a_0 = 0$, $a = 1$, the gain $\gamma = 0$ as well as the coefficients are all constants. Equation (1) then reduces to the standard CQNLS equation, which leads to the standard bright and dark solitary wave solutions to Eq. (1).

(ii) *Periodic solitary waves.* As a general case, we choose $a_0 = 0.1$, $\omega_1 = 1$. The coefficients are then trigonometric forms of time, and Eq. (1) has periodic oscillating bright and dark solitary wave solutions, as plotted in Figs. 1(a) and 1(b), respectively. One can see that the solitary waves maintain the same widths but change in their amplitudes (proportional to $\sqrt{a}$) with the increasing time.

Obviously, the Hamiltonian $\mathcal{H}$ in the case (i) is conserved while is not in case (ii) [Eq. (13) is not satisfied]. Thus, model (1) in the above two cases is important both in nonlinear optics and BECs [14,32,33], and the results are applicable for these systems.

B. Space-quadratic potential [$F(\xi) = F_0$]

We now address solutions to Eq. (1) when $F(\xi)$ is a real constant, that is, $F(\xi) = F_0$. In this case, $q_3(\xi,t) = q_4(\xi,t) = 0$, $q_1(\xi,t)$, and $q_2(\xi,t)$ are only the functions of time [$q_1(\xi,t) = $
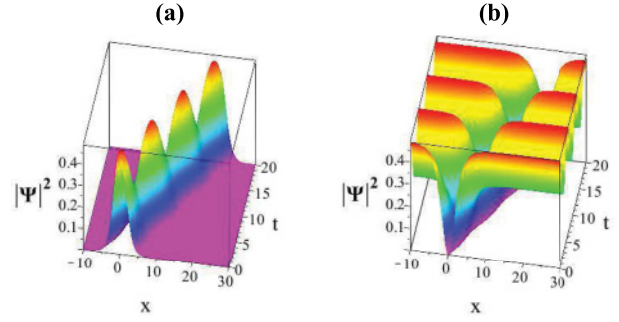

FIG. 1. (Color online) Periodic solitary wave solutions of Eq. (1), in the case of a vanishing potential and time-dependent coefficients. (a) Bright solitary wave solution for $g_0 = 1$, $N = 0.5$, $w = 1$, and (b) dark solitary wave solution for $g_0 = -1$, $N = 2$, $w = -1$. The other parameters are $\beta_0 = 1$, $T_0 = 0$, $\alpha_0 = 1$, $F_0 = 1$, $a_0 = 0.3$, and $\omega_1 = 1$.

$q_1(t), q_2(\xi,t) = q_2(t)]$, and the parameter $X(x,t)$ has the form of $F_0\alpha(t)x$. Thus, we can obtain the SQ potential

$$V_{SQ}(x,t) = \theta^2(t)x^2, \quad (15)$$

where $\theta^2(t) = q_1(t) + \frac{q_2(t)}{2} = \frac{1}{2}a^{-2}g_0 F_0^2\alpha(a_t\alpha_t - a\alpha_{tt})$. It is known that the SQ potential has been interestingly discussed [22,24,27,28] and is important to realize BEC in experiments. Moreover, from Eqs. (6) and (7) we can see the coefficients in Eq. (1) are time-dependent functions, and phase is a quadratic profile. In this case, Eq. (1) becomes the generalized nonautonomous CQNLS equation with time-dependent coefficients

$$i\frac{\partial\psi}{\partial t} + f(t)\frac{\partial^2\psi}{\partial x^2} + g(t)|\psi|^2\psi + G(t)|\psi|^4\psi$$
$$+ \theta^2(t)x^2\psi + i\gamma(t)\psi = 0, \quad (16)$$

where $f(t), g(t), G(t), \gamma(t)$ satisfy Eq. (4) and Eq. (6) and Eqs. (7) for $F(\xi) = F_0$.

Equation (16) can be associated with two main physical problems: (i) beam propagation in a graded-index waveguide with periodical structure [34] and (ii) nonlinear waves of BECs inside a periodical potential via dispersion management using the concept of effective mass [35]. In particular, when $\theta^2(t) = 0$, the potential is vanishing and Eq. (16) can describe the evolution of nonlinear optical pulses in CQ nonlinear media, which has already been discussed in Ref. [14].

Generally, Eq. (16) is not integrable. Having in mind the solvable conditions (6) and (7), we have:

$$f(t) = \frac{a}{2g_0\alpha^2 F_0^2}, \quad G(t) = \frac{G_0\alpha^2 F_0^2}{g_0 a}, \quad (17a)$$

$$\gamma = \frac{\alpha_t}{\alpha} - \frac{g_0^2 f_t G}{G_0} - \frac{g_t}{g}. \quad (17b)$$

That is, exact solitary wave solutions of Eq. (16) can exist under Eqs. (17).

Now we focus on three different SQ potentials.

1. Decaying bent solitary waves

We first consider the SQ potential without time modulation by taking $a = \alpha^2, \theta^2(t) = \lambda$, where λ is a constant. This choice

leads us to $\alpha = \frac{2C_0 e^{C_0 t}}{C_1 e^{2C_0 t} - C_2}$, where $C_0 = \sqrt{\frac{2\lambda}{g_0 F_0}}$, C_1, and C_2 are arbitrary real constants. With this, the potential has the form

$$V_{SQ1}(x,t) = \lambda x^2. \tag{18}$$

In this case, the coefficients f, G are constants, g is a function of time, and the gain γ is vanishing. With this, we can use Eq. (5a) to find $\rho(x,t) = \sqrt{\alpha/F_0}$.

Now, with the parameters shown above, the solitary wave solutions can be obtained according to Eqs. (11) and (12). It is noted that one can obtain decaying bent solitary waves by selecting special values for C_1 and C_2. As an example, we choose the parameters $C_1 = 1$ and $C_2 = -1$, and with this we have $\alpha = C_0 \text{sech}(C_0 t)$, which acquires $g_0 > 0, F_0 > 0$ or $g_0 < 0, F_0 < 0$, respectively. The intensity of the bright decaying bent solitary wave is given by

$$|\psi_B(x,t)|^2 = \frac{C_0 M^2 \text{sech}(C_0 t)}{g_0 F_0}$$
$$\times \{1 + N \cosh[p(X - wT)]\}^{-1}, \tag{19}$$

where $X = F_0 C_0 \text{sech}(C_0 t)x$ and $T = g_0^{-1} C_0 \tanh(C_0 t) + T_0$.

In Fig. 2, we plot the decaying bent solitary waves to show how they behave as functions of space and time. Figures 2(a) and 2(b) demonstrate the intensity profiles of ψ_B and ψ_D, respectively. Figures 2(c) and 2(d) show the width $\frac{1}{pF_0\alpha(t)}$, amplitude $\frac{M}{\sqrt{1+N}}\sqrt{\frac{\alpha(t)}{g_0 F_0}}$, and velocity of the wave center $v_c = w(g_0 F_0)^{-1}[\alpha - \alpha^{-2}\alpha_t(\int_0^t \alpha(t')^2 dt' + T_0 g_0)]$ of the solitary wave given by Eq. (19). It is observed that the width of the solitary wave becomes wide but amplitude becomes small as time goes on. The velocity of the solitary wave increases as an exponential, depending on the changes of the parameter α.

Therefore, the solitary wave displays broadening and moving behavior with the increasing time. As a result, one can make the solitary wave broaden in a predictable fashion by designing the form of $\alpha(t)$ according to its expression. Broadening of the solitary wave is also studied in Ref. [36].

2. Snakelike solitary waves

Consider $a_0 = 0$ and α to be the function of trigonometric form as noted in Eq. (14). As mentioned, we see that the coefficients f, G, γ are functions of time. In this case, the parameter $\rho(x,t) = 1/\sqrt{\alpha F_0}$ and variable $\xi = [1 + \epsilon \cos(\omega_0 t)]x$. Now, the potential is in the form

$$V_{SQ2}(x,t) = \tfrac{1}{4}\epsilon g_0 \omega_0^2 F_0^2 [\epsilon + 2\cos(\omega_0 t) + \epsilon\cos(2\omega_0 t)]x^2. \tag{20}$$

This potential is modulated by a time-periodic optical superlattice, which includes two different frequencies (ω_0 and $2\omega_0$) [37]. It changes from attractive to expulsive behavior periodically, as we show in Fig. 3(a). Recently, Belmonte-Beitia and Calvo obtained similar results [24].

(a)

(b)   **(c)**

(d)   **(e)**

FIG. 3. (Color online) Plots of (a) the SQ potential expressed by Eq. (20) with $\omega_0 = 1, \epsilon = 0.5$. (b) $|\psi_B|^2$ and (c) $|\psi_D|^2$ corresponding to potential (20) for $\omega_0 = 1, \epsilon = 0.3$. (d) The width $\frac{1}{pF_0\alpha(t)}$ (upper line) and amplitude $\frac{M}{\sqrt{1+N}}\frac{1}{\sqrt{g_0 F_0\alpha(t)}}$ (lower line) and (e) the velocity of the wave center v_c of the solution (21). The other parameters are the same as those used in Fig. 1.

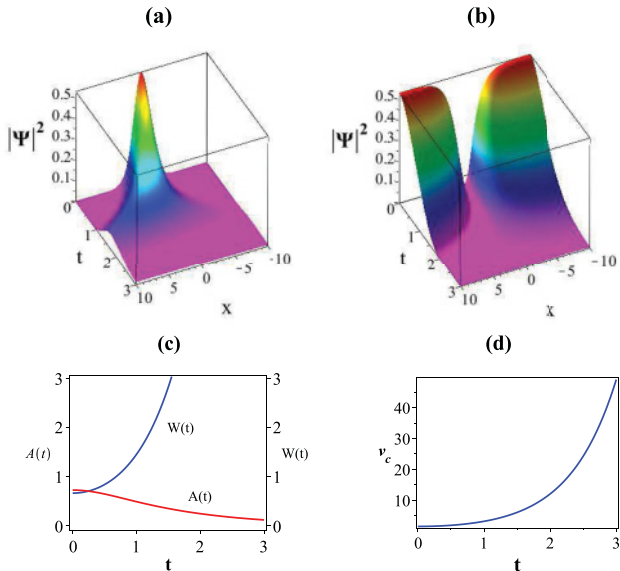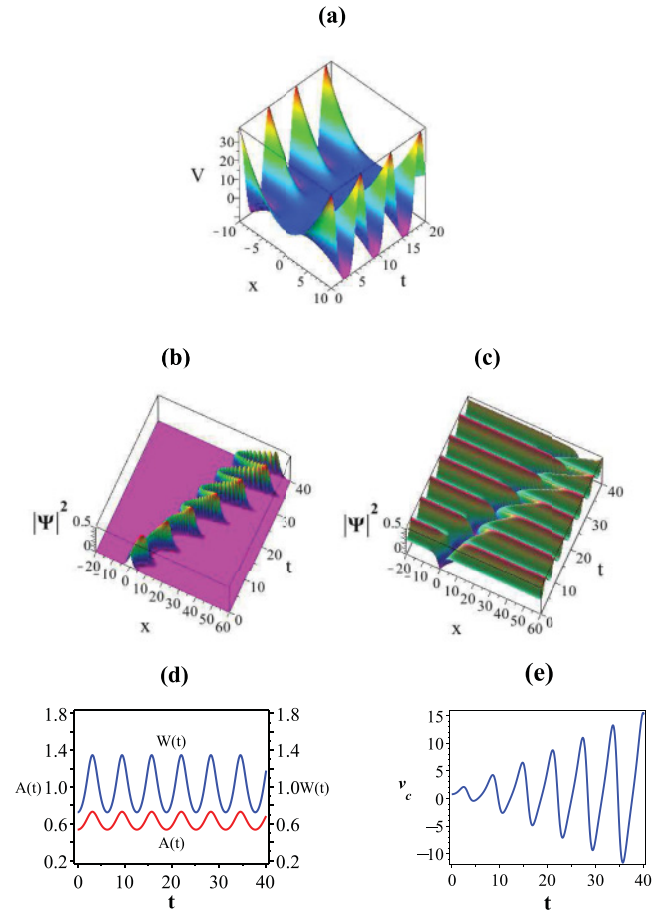**(a)**   **(b)**

(c)   **(d)**

FIG. 2. (Color online) Plots of (a) $|\psi_B|^2$ and (b) $|\psi_D|^2$ with the potential depicted by Eq. (18) for $\lambda = 1, C_1 = 1, C_2 = -1$. (c) The width $\frac{1}{pF_0\alpha(t)}$ (upper line) and amplitude $\frac{M}{\sqrt{1+N}}\sqrt{\frac{\alpha(t)}{g_0 F_0}}$ (lower line) and (d) the velocity of the wave center v_c of the solution (19). Here, and in other figures, $W(t)$ and $A(t)$ represent the widths and amplitudes of the solutions, respectively. The other parameters are the same as those used in Fig. 1.

Solitary waves under potential (20) demonstrate snakelike behavior. We take the bright snakelike solitary wave as an example to illustrate how it behaves as a function of x and t. Its intensity is given by

$$|\psi_B(x,t)|^2 = \frac{M^2}{g_0 F_0[1 + \epsilon \cos(\omega_0 t)]}$$
$$\times \{1 + N \cosh[p(X - wT)]\}^{-1}, \quad (21)$$

where $X = F_0[1 + \epsilon \cos(\omega_0 t)]x$, $T = g_0^{-1}t + T_0$.

In Fig. 3, we plot the dynamics of the snakelike solitary waves. Figures 3(b) and 3(c) demonstrate the intensity profiles of the wave functions ψ_B and ψ_D, respectively. Figures 3(d) and 3(e) show the width $\frac{1}{pF_0\alpha(t)}$, amplitude $\frac{M}{\sqrt{1+N}} \frac{1}{\sqrt{g_0 F_0\alpha(t)}}$, and velocity of the wave center $v_c = w(g_0 F_0)^{-1}[\alpha^{-1} - \alpha^{-2}\alpha_t(t + T_0 g_0)]$ of the solitary wave given by Eq. (20). The center position of the solitary wave is $x_c = w(F_0\alpha)^{-1}(g_0^{-1}t + T_0)$, which leads a snakelike effect of the solitary wave. As one can see from Figs. 3(d) and 3(e), with the increasing time, the solitary wave displays a periodic change in the width and amplitude, and the velocity of the wave center executes periodic oscillations and an increase in the magnitude.

3. Formation of two bound-state solitary waves

Considering the trapping potential, which is related to parametric amplification of elementary excitations of nonlinear media [38] and studied in Refs. [22,24,25], in order to obtain the trapping potential, we take $a = \alpha^2$ and define $\chi = 1/\alpha$, and then we have the Mathieu equation $d^2\chi/dt^2 - (2/g_0 F_0^2)\theta^2(t)\chi = 0$ with $\theta^2(t) = 1 + \varepsilon \cos(\theta_0 t)$. Now the trapping potential is given by

$$V_{SQ3}(x,t) = [1 + \varepsilon \cos(\theta_0 t)]x^2 \quad (22)$$

with $\varepsilon \in (-1,1)$ and $\theta_0 \in \mathbb{R}$. We plot this potential in Fig. 4(a). In order to investigate the exact solutions of Eq. (1), we choose parameters $g_0 = F_0 = \theta_0 = 1$ and $\varepsilon = 0.5$. In this case, the solution of the above Mathieu equation is $\chi = AC_M(-8,2,t/2) + BS_M(-8,2,t/2)$, where A and B are constants and C_M and S_M refer to the cosine and sine Mathieu functions, respectively. It is interesting that one obtains the explicit expression of bound states of solitary waves according to Eq. (11). Figure 4(b) shows the formation of two bound-state solitary waves in the trapping potential with $A = B = 1$.
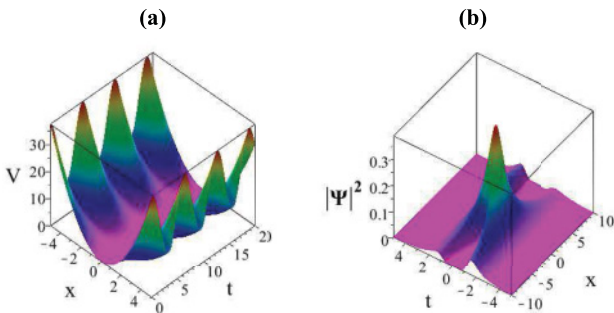

FIG. 4. (Color online) (a) Plot of the trapping potential given by Eq. (22) with $\theta_0 = 1$, $\varepsilon = 0.5$. (b) Two solitary waves in bound-state formation.

Investigations of similar structures in optical fibers with a variable dispersion have been seen in Ref. [39].

In keeping with the experiments, we discuss the applications of our above results in the BECs. In cases 1 and 3, the dispersion management parameter $f(t)$ is a constant (can be set as 1), and the gain γ is vanishing. Furthermore, we can obtain that the Hamiltonian $\mathcal{H}$ in the two cases is conserved in light of Eq. (13). Thus, the norm $\int_{-\infty}^{\infty} |\psi|^2 dx = \text{const} \equiv \mathcal{N}$ denotes the particle number of atoms in BECs. According to the theory of Feshbach resonance, the behavior of the scattering lengths in the vicinity of a Feshbach resonance can be written as $a_s(t) = a_{bg}[1 + \Delta/(B_0 - B(t))]$, and so $g(t) = a_s(t)/a_{bg} = 1 + \Delta/[B_0 - B(t)]$, with a_{bg} is the background scattering length, B_0 is the resonant value of the magnetic field, and Δ is the width of the resonance. Therefore, the magnetic field $B(t)$ reads $B(t) = B_0 + \Delta/[1 - g(t)]$, which varies with $g(t)$. In these two cases, we have $g(t) = F_0\alpha(t)$. Thus, by choosing $\alpha(t)$, the Feshbach resonance management is realized easily. This effect provides a direct and simple way to compress the soliton and obtain formation of two solitary waves bound states. As for case 2, the solitary waves can exist under the dispersion management in BECs once a controlled variation of the effective mass would be possible.

C. Optical lattice potential $[\alpha(t) = \alpha_0]$

In recent years optical lattices have been suggested as an important tool for controlled manipulation of stable, spatially localized nonlinear waves [40]. Theoretical investigations of solitons, trapped in a rapidly driven asymmetric one-dimensional optical lattice, have shown that their mass-dependent transport could be available in such an "optical ratchet" [41].

On the basis of this motivation, in this subsection, we will show how solitary waves propagate in the Fourier-synthesized lattice potential (a ratchet potential). It is interesting that such lattice potential can be obtained explicitly according to Eq. (8) by appropriately selecting the parameters $a(t)$ and $F(\xi)$. When $\alpha(t) = \alpha_0$, we get $q_1(\xi,t) = q_2(\xi,t) = q_3(\xi,t) = 0$, where $q_4(\xi,t)$ is a function both in space and time. Thus, the potential takes the form $V(x,t) = q_4(\xi,t)$. Moreover, this yields the phase $\phi(x,t) = 0$ since we choose the integral function of time in Eq. (5c) to be zero. To obtain the lattice potential, we take $F(\xi) = 1/[\upsilon + \upsilon_0 \cos(\omega_2\xi)]$ in Eq. (8), with $\upsilon_0 \in (-\upsilon,\upsilon)$, $\omega_2 \in \mathbb{R}$ and υ as a positive constant. The so-called Fourier-synthesized lattice potential now is given by

$$V_{OL}(x,t) = [V_0 + V_1 \cos(\omega_2\xi) + V_2 \cos(2\omega_2\xi)]a(t), \quad (23)$$

where $V_0 = 3\upsilon_0^2\omega_2^2/16$, $V_1 = \upsilon_0\upsilon\omega_2^2/4$, $V_2 = \upsilon_0^2\omega_2^2/16$, and $\xi = \alpha_0 x$, and $a(t)$ is a periodic function given by Eq. (14). One can see that V_1 and V_2, related to the depths of the biperiodical lattice potential, depend on υ and υ_0. In the experiments of cold atomic beam for interferometry, they are proportional to the laser intensity and inverse with detuning from atomic resonance [42]. In Ref. [19] the authors also demonstrated this ratchet potential to describe a periodical modulation of the refractive index modulated in both transverse and longitudinal directions in the resonator and obtained a novel type of Bloch cavity solitons. Thus, Eq. (1) trapped in potential (23) may be realized in such nonlinear media where both transverse
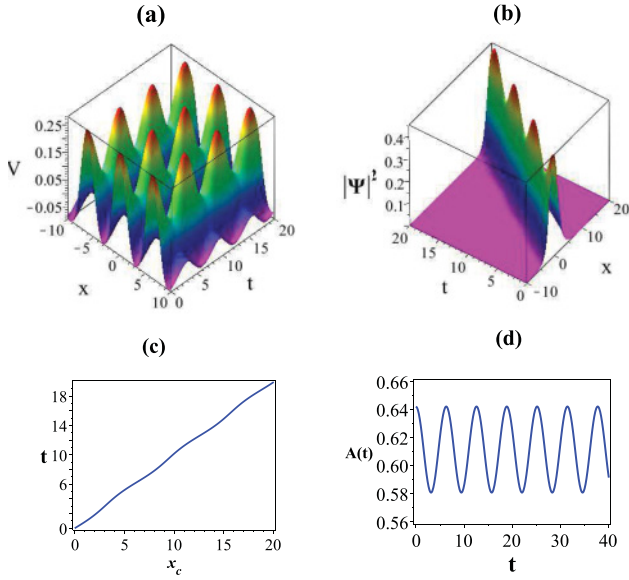
FIG. 5. (Color online) (a) Plot of the OL potential given by Eq. (23) with parameters $\upsilon = \omega_1 = \omega_2 = 1, a_0 = \upsilon_0 = 0.5$. (b) Evolution of the bright solitary wave in potential (23). (c) Center position and (d) amplitude of the solution (24). The parameters are $a_0 = \upsilon_0 = 0.1$.

and longitudinal directions show nonuniform distribution. Further, a similar potential has also been studied for the NLS equation [43].

Parameters of the Fourier-synthesized lattice potential (23) can be determined by appropriately choosing the function $a(t)$ and the lattice harmonics V_1, V_2. The stationary potential of the form (23)($a_0 = 0$) both in BECs and nonlinear waveguide has also been studied in Ref. [44]. We plot the Fourier-synthesized lattice potential in Fig. 5(a) with the parameters $\upsilon = \omega_1 = \omega_2 = 1$, $a_0 = \upsilon_0 = 0.5$. As can be seen, this potential resembles a periodic sequence of hills in the transverse and longitudinal directions. Using Eq. (5a) we can get $\rho(x,t) = \sqrt{\Lambda/\alpha_0}$, if we define $\Lambda = [\upsilon + \upsilon_0 \cos(\omega_2 \xi)][1 + a_0 \cos(\omega_1 t)]$, thus $\alpha_0 > 0$. We see from Eqs. (7) that the coefficients f, G are the functions of space and time, g is a function of x, and γ is time dependent.

According to Eqs. (11) and (12), solutions of Eq. (1) under the OL potential can be obtained. Taking the bright solitary wave as an example

$$|\psi_B(x,t)|^2 = \frac{M^2 \Lambda}{g_0 \alpha_0} \{1 + N \cosh[p(X - wT)]\}^{-1}, \quad (24)$$

where $X = \int_0^\xi [\upsilon + \upsilon_0 \cos(\omega_1 \xi')]^{-1} d\xi'$ and $T = g_0^{-1}[t + \frac{a_0}{\omega_2} \sin(\omega_2 t)] + T_0$. In Fig. 5(b), we display the dynamics of the bright solitary wave with $a_0 = \upsilon_0 = 0.1$. It is obvious that the solitary wave exhibits periodic oscillation along with the increasing time while its width remains unchanged.

In our solution, the center position of the solitary wave can be determined by $X(x_c) = wT$. This leads to a relationship between wave center x_c and time t, as we plot in Fig. 5(c). It is found that the wave center swings around instead of propagating in a straight line. In Fig. 5(d), we demonstrate the amplitude (proportional to $\sqrt{\Lambda}$) of the solution (24) to illustrate how it varies with respect to time. Note that the

dark solitary wave solution can also be obtained according to Eq. (12); we do not show here to avoid tedium. When $a_0 = 0$, corresponding to the stationary form of Eq. (23), f, g, and G are only related to coordinate x, and the gain γ is vanishing. It is expected that, in this case, solitary wave solutions will be existence in the presence of a segment with modified dispersion and/or nonlinearity [45]. Furthermore, when $a_0 = \upsilon_0 = 0$, the solitary waves evolve into the standard types that have no oscillation. It is important to stress that one can control the shapes of the solitary waves through the action of the lattice management. For example, one can design the evolution of the solitary wave's peak and the wave center's motion through the parameters υ, υ_0, and a_0 related to the depths of the Fourier-synthesized lattice potential according to the relationship depicting the wave center as mentioned. We hope this result will be valuable to design an OL potential that is expected to produce the bright or dark solitons.

We have demonstrated that the exact solitary wave solutions can be constructed in model (1) with the Fourier-synthesized lattice potential. In Sec. III E, the stability of the solution is checked under slight disturbance of the constraint conditions and the initial perturbation of white noise, and the results show that the solitary waves still propagate in a stable way. To our knowledge, solitons in OLs are usually found in a numerical form, with rarely analytical results [46]. Therefore, we hope our results will be useful for the further study in optical communications and relative subjects and stimulate novel experiments in the field.

D. Potential barrier (well) and flying bird potential

We have thus far been very specific in choosing the cubic nonlinearity $g(x,t)$. However, in order to show the general properties of Eq. (1), we should consider $g(x,t)$ as a function both in space and time. A specific cubic nonlinearity in the case of BECs with controlled optical interactions [22,24,25] may simulate interesting external potential and solutions for our model (1) and is given explicitly by

$$g(x,t) = \alpha e^{\xi^2/b^2}, \quad (25)$$

where b is a real constant. Therefore, Eq. (25) may be exist in the nonlinear media when its transverse and longitudinal directions are nonuniform distribution. We consider the special case $a_0 = 0$, and α is the trigonometric form mentioned in Eq. (14). With this choice we have $F(\xi) = e^{\xi^2/b^2}$ and $\rho(x,t) = \sqrt{\alpha^{-1} e^{-\xi^2/b^2}}$. The potential is given as follows:

$$V(x,t) = l(t) + h_1(\xi,t)e^{2\xi^2/b^2} + h_2(\xi,t)e^{-2\xi^2/b^2}, \quad (26)$$

with

$$l(t) = \frac{g_0 b^2}{4\alpha^2}(\alpha\alpha_{tt} - \alpha_t^2),$$

$$h_1(\xi,t) = \frac{g_0 b^2[\alpha_t^2(1 - 2\xi^2/b^2) - \alpha\alpha_{tt}]}{4\alpha^2},$$

$$h_2(\xi,t) = \frac{1 + \xi^2/b^2}{2g_0 b^2}.$$

This potential exhibits very different features for the choice of ϵ, in spite of the apparent complexity of its expression.
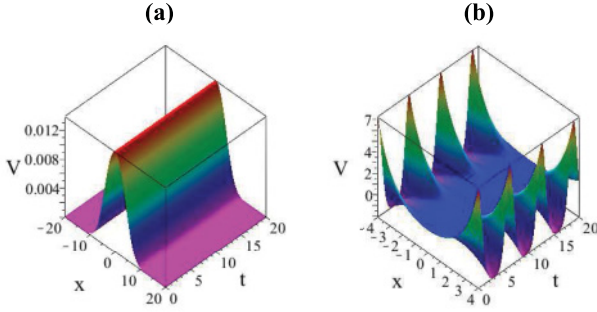
FIG. 6. (Color online) Plots of the potential given by Eq. (26) with (a) $\epsilon = 0$ and (b) $\epsilon = 0.3$. The other parameters are $\omega_0 = g_0 = 1$, $b = 6$.

When $\epsilon = 0$, it becomes potential barrier (well); when $\epsilon \neq 0$, it represents FB behavior.

1. Potential barrier (well)

When $\epsilon = 0$, $\alpha = 1$, potential (26) becomes

$$V(x,t) = \frac{1 + x^2/b^2}{2g_0 b^2} e^{-2x^2/b^2}. \quad (27)$$

This potential represents the potential barrier or well, depending on the sign of g_0. When $g_0 > 0$, it represents the potential barrier; when $g_0 < 0$, it represents the potential well. Thus, solutions of Eq. (1) are the bright types in potential barrier while dark types in potential well. We plot the potential barrier in Fig. 6(a) with $\omega_0 = g_0 = 1$, $b = 6$. The corresponding bright solitary waves are decaying with respect to time, as plotted in Fig. 7(a) with $w = 2$, $b = 6$. One can see that the potential barrier influences the shape of the solitary wave that decays with the increasing time. As for the potential well, the corresponding dark solitary waves are also decaying.

2. Flying bird potential

If $\epsilon \neq 0$, (26) represents an FB potential. This potential periodically varies in time with attractive and expulsive sign-reversible characteristics, as we plot in Fig. 6(b). This characteristics is related to the sign of g_0 which controls the cubic nonlinearity and determines the solitary wave solution that is bright or dark. Moreover, the potential represents periodic and quasiperiodic behaviors depending on the choice of the parameter ω_0. For example, if we take $\omega_0 = \sqrt{2}$ in Eq. (26), we can obtain quasiperiodic potential. When $b \to \pm\infty$, the potential is vanishing. Unlike in Sec. III A, coefficients of (1) are the functions of space and time in this case.

Solutions of Eq. (1) with the FB potential can be obtained from Eqs. (11) and (12). We consider the bright solitary wave which changes like a snake with amplitude decays

$$|\psi_B(x,t)|^2 = \frac{M^2 e^{-\xi^2/b^2}}{g_0[1 + \epsilon \cos(\omega_0 t)]}$$
$$\times \{1 + N \cosh[p(X - wT)]\}^{-1}, \quad (28)$$

with $X = \frac{b\sqrt{\pi}}{2}\text{erfi}(\frac{\xi}{b})$ and $T = g_0^{-1}t + T_0$, where $\text{erfi}(s) = \frac{2}{\sqrt{\pi}}\int_0^s e^{\tau^2}d\tau$ is called an imaginary error function. We plot
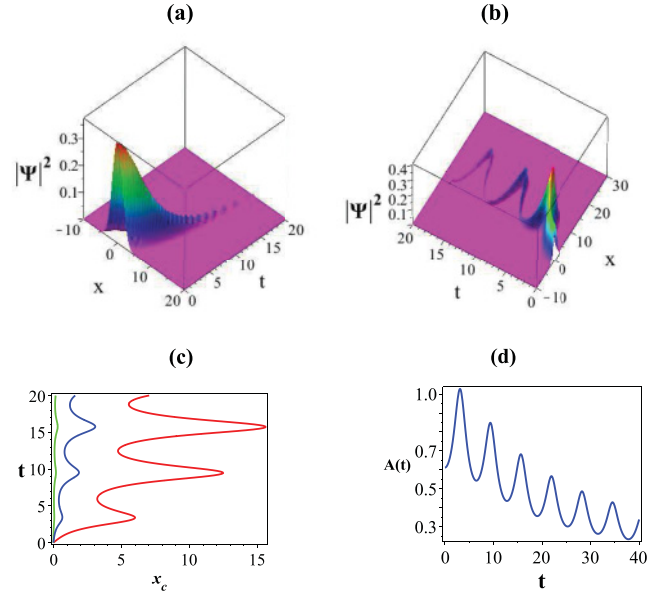

FIG. 7. (Color online) The decaying solitary wave of Eq. (1) with (a) $\epsilon = 0$, and (b) $\epsilon = 0.5$ for $w = 2$, $b = 6$, corresponding to potential barrier and FB potential, respectively. (c) Center position of the solution (28) with $w = 0.01$ (left line), $w = 0.1$ (middle line), and $w = 1$ (right line). (d) Amplitude of the solution (28) with $w = 0.5$.

the intensity of ψ_B in Fig. 7(b). One can see that the wave packet presents time periodic movement, with the amplitude increasing and decreasing periodically but overall decreasing.

In our solution, both the amplitude, center position, and speed of the wave packet vary with time and space. It is therefore difficult to find explicit expressions between x and t. But we can plot them according to their relationship and then study their properties. The wave center position satisfies the equation $X - wT = 0$, that is,

$$\frac{b\sqrt{\pi}}{2}\text{erfi}\left\{\frac{[1 + \epsilon \cos(\omega_0 t)]x_c}{b}\right\} - w(g_0^{-1}t + T_0) = 0 \quad (29)$$

is plotted in Fig. 7(c) with $w = 0.01, 0.1$, and 1. It is shown that the wave center shows a large swing around away from $x = 0$ for big w, while almost no swing nearby $x = 0$ for small w. This is because when w is small, the wave packet is confined in the vicinity of $x = 0$.

The evolution of the amplitude can be described by

$$A_{\psi_B} = M e^{(1+\epsilon\cos(\omega_0 t))x_c^2/2b^2}\{g_0(1+N)[1+\epsilon\cos(\omega_0 t)]\}^{-\frac{1}{2}}, \quad (30)$$

where x_c satisfies the Eq. (29). One can see that the parameters ϵ, ω_0, N, T_0, g_0, and b all affect the amplitude, which leads to the complex changes of the solitary wave. We plot the dynamics of the amplitude in Fig. 7(d) with $w = 0.5$. It is observed that the amplitude presents a periodic increase and decrease, but overall is a decrease. Similar to the amplitude, we note that the width of the wave also demonstrates a periodic increase and decrease.

From the discussions above, we can see that solitary waves are all decaying in both FB potential and potential
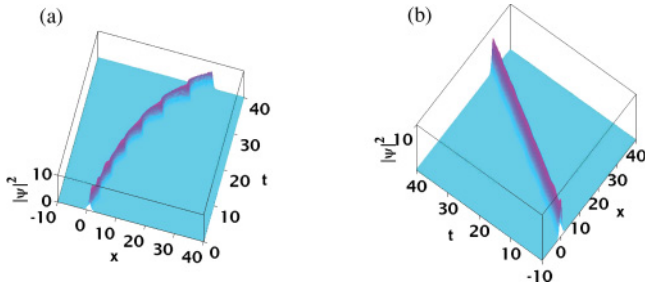
FIG. 8. (Color online) The numerical evolution of the exact solution (21) (a) and (24) (b) under the perturbation in the constraint conditions. The parameters for solution (21) are $f = 0.9 \times 0.5 g_0^{-1} F_0^{-2} [1 + \epsilon \cos(\omega_0 t)]^{-2}$ and $\epsilon = 0.16$, $\beta_0 = 0.1$, $w = 0.5$, while for solution (24) the parameters are $f = 0.9 \times 0.5 g_0^{-1} \alpha_0^{-2} \Lambda[\upsilon + \upsilon_0 \cos(\omega_2 \xi)]$ and $a_0 = 0$, $\upsilon_0 = 0.2$, $\beta_0 = 0.1$, $w = 0.8$. The other parameters are the same as those used in Figs. 3(b) and 5(b).

barrier (well), and hence the solitary waves are unstable. This situation will be changed if one chooses the parameter $w = 0$. In this case, solution of the autonomous CQNLS equation [Eqs. (9) and (10)] is in the stationary form, and the solution of Eq. (1) is no longer decaying with respect to time.

E. Stability of the solitary wave solutions

Thus far, we have obtained the exact solitary wave solutions under the constraint conditions (6)–(8) which provide the balances among the management coefficients in model (1). In real applications, however, it may be difficult to produce exactly such constraint conditions. Therefore, a study for the perturbations in the constraint conditions (6)–(8) is necessary. Here we take the solutions (21) and (24) as examples and disturb the constraint conditions in the way: $f = 0.9 \times 0.5 g_0^{-1} F_0^{-2} [1 + \epsilon \cos(\omega_0 t)]^{-2}$ for solution (21) and $f = 0.9 \times 0.5 g_0^{-1} \alpha_0^{-2} \Lambda[\upsilon + \upsilon_0 \cos(\omega_2 \xi)]$ for solution (24), and the other conditions do not change. Results of numerical calculations are shown in Fig. 8. We can see that the solitary waves present the stable state in Fig. 8(a) while propagate stably in Fig. 8(b) after a short adjustment. In addition to this, we have made more numerical calculations for the constraint conditions by perturbing other management coefficients and the results show that the solitary waves still propagate in a
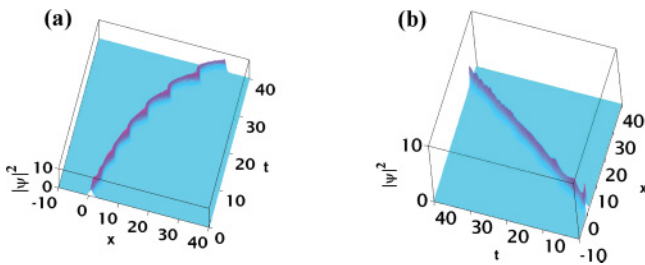

FIG. 9. (Color online) The numerical evolution of the exact solution (21) (a) and (24) (b) under the initial perturbation of white noise. The initial data for solution (21) are $\epsilon = 0.16$, $\beta_0 = 0.1$, $w = 0.5$, while for solution (24) they are $a_0 = 0$, $\upsilon_0 = 0.2$, $\beta_0 = 0.1$, $w = 0.8$. The other parameters are the same as those used in Figs. 3(b) and 5(b).

stable way. Therefore, the evolution of the solitary waves is not sensitive to the perturbations in the constraint conditions. As a result, it is possible to relax the limitations to the constraint conditions. This may make the soliton control technique more realistic and provide prospects for applications in the future.

Finally, we briefly analyze the stability of the solitary wave solutions found above. We still take the solutions (21) and (24) as examples to perform numerical experiments of Eq. (1). We add white noise in the pulse $\psi(x,0)$, then the perturbed pulse reads

$$\psi_{\text{pert}} = \psi(x,0)[1 + 0.1 \text{random}(x)]. \qquad (31)$$

The numerical results are shown in Figs. 9(a) and 9(b). The results demonstrate that the solitary waves can propagate in a stable way under the initial perturbation of white noise. It is noted that the solitary wave expressed by Eq. (24) shows smaller changes in the wave's peak during the propagation comparing with its analytical profiles, which caused by the numerical simulation technique. These results may useful in study of propagation of pulses in femtosecond fiber systems or optical communication links with distributed dispersion and nonlinearity management and the presence of gain (loss).

Although we have displayed here the results of stability study only for two examples of model (1), similar conclusions hold for other solutions as well.

IV. CONCLUSIONS

In conclusion, we have solved analytically the generalized nonautonomous CQNLS equation by using the similarity transformation. By choosing special forms of the cubic nonlinearity $g(x,t)$ based on $\alpha(t)$ and $F(\xi)$, a simple procedure is established to obtain different classes of potentials and solutions. The solutions exist under certain conditions and impose constraints on the coefficients depicting dispersion, CQ nonlinearities, and gain (or loss). In this way, Eq. (1) can reduce to the standard CQNLS equation and the generalized nonautonomous CQNLS equation with time-dependent coefficients, and the conservation condition of the Hamiltonian $\mathcal{H}$ is presented. Following, a meaningful result is obtained that a more general expression of the external potential, which not only contains the case in previous literature [26] but also simulates some interesting periodic potentials, such as the SQ potential, OL potential, FB potential, and potential barrier (well). It is noted that one can also obtain other potentials according to the expression of the external potential by appropriately selecting the parameters $a(t)$, $\alpha(t)$, and $F(\xi)$. Then, abundant of exact solitary wave solutions have been found under these different types of external potentials, including decaying solitary waves, snakelike solitary waves, and solitary waves in an OL potential. Properties of some solutions are also studied intensively, including the influence of the arbitrary time-dependent function $a(t)$ on the potentials and solutions, and the control of the widths, amplitudes, speeds, and center positions of some solitary waves. Finally, the stability of the solitary waves under slight disturbance of the constraint conditions and initial perturbation of white noise is discussed numerically; the results reveal that the solitary waves can propagate in a stable way under slight disturbance of the constraint conditions and the initial perturbation of white

noise. We believe that the produce of designing nonlinearities and potentials in this paper can also apply to studying generalized nonautonomous cubic NLS equations, high-dimensional situations, multicomponent systems, and nonlinear optical systems.

[1] R. K. Dodd, J. C. Eilbeck, J. D. Gibbon, and H. C. Morris, *Solitons and Nonlinear Wave Equations* (Academic Press, New York, 1982).

[2] C. De Angelis, IEEE J. Quantum Electron. **30**, 818 (1994); S. Gatz and J. Herrmann, Opt. Lett. **17**, 484 (1992).

[3] S. Inouye, M. R. Andrews, J. Stenger, H.-J. Miesner, D. M. Stamper-Kurn, and W. Ketterle, Nature (London) **392**, 151 (1998); F. Kh. Abdullaev, A. Gammal, L. Tomio, and T. Frederico, Phys. Rev. A **63**, 043604 (2001); E. Braaten and H. W. Hammer, Phys. Rev. Lett. **87**, 160407 (2001).

[4] *Future Directions of Nonlinear Dynamics in Physical and Biological Systems*, edited by P. L. Christiansen, NATO ASI, Ser. B, Vol. 312 (Plenum Press, New York, 1993); A. R. Bishop and T. Schneider, *Solitons and Condensed Matter Physics* (Springer-Verlag, Berlin, 1978); M. J. Ablowitz and P. A. Clarkson, *Solitons, Nonlinear Evolution Equations and Inverse Scattering* (Cambridge University Press, Cambridge, UK, 1991); A. C. Newell and J. V. Moloney, *Nonlinear Optics* (Addison-Wesley, Redwood City, CA, 1992).

[5] R. Camassa, J. M. Hyman, and B. P. Luce, Physica D **123**, 1 (1998); V. E. Zakharov and A. B. Shabat, Zh. Eksp. Teor. Fiz. **61**, 118 (1971); Sov. Phys. JETP **34**, 62 (1972); A. Scott, F. Chu, and D. McLaughlin, Proc. IEEE **61**, 1443 (1973); D. J. Kaup and A. C. Newell, Proc. R. Soc. London A **361**, 413 (1978); V. Makhankov, Phys. Rep. **35**, 1 (1978).

[6] A. Hasegawa and Y. Kodama, *Solitons in Optical Communications* (Oxford University Press, New York, 1995); L. F. Mollenauer and J. P. Gordon, *Solitons in Optical Fibers* (Academic Press, Boston, 2006); J. R. Taylor, *Optical Solitons-Theory and Experiment* (Cambridge University Press, Cambridge, UK, 1992).

[7] G. P. Agrawal, *Nonlinear Fiber Optics* (Academic Press, San Diego, CA, 2001), 3rd ed.; N. N. Akhmediev and A. Ankiewicz, *Solitons:Nonlinear Pulses and Beams* (Chapman & Hall, London, 1997).

[8] V. N. Serkin, A. Hasegawa, and T. L. Belyaeva, Phys. Rev. Lett. **98**, 074102 (2007).

[9] R. Y. Hao, R. C. Yang, L. Li, and G. S. Zhou, Opt. Commun. **281**, 1256 (2008); R. Y. Hao, G. S. Zhou, *ibid.* **281**, 4474 (2008); Y. Wang and R. Y. Hao, *ibid.* **282**, 2995 (2009); Q. Y. Li, Z. D. Li, S. X. Wang *et al.*, *ibid.* **282**, 1676 (2009).

[10] X.-J. Lai and J.-F. Zhang, Z. Naturforsch A **64**, 347 (2009).

[11] H. G. Luo, D. Zhao, and X. G. He, Phys. Rev. A **79**, 063802 (2009); A. Kundu, Phys. Rev. E **79**, 015601(R) (2009).

[12] P. Béjot, J. Kasparian, S. Henin, V. Loriot, T. Vieillard, E. Hertz, O. Faucher, B. Lavorel, and J.-P. Wolf, Phys. Rev. Lett. **104**, 103903 (2010); D. Novoa, H. Michinel, and D. Tommasini, *ibid.* **105**, 203904 (2010); V. Loriot, E. Hertz, O. Faucher, and B. Lavorel, Opt. Express **17**, 13429 (2009).

[13] L. Bergé, V. K. Mezentsev, J. J. Rasmussen, P. L. Christiansen, and Yu. B. Gaididei, Opt. Lett. **25**, 1037 (2000).

[14] K. Senthilnathan, Q. Li, K. Nakkeeran, and P. K. A. Wai, Phys. Rev. A **78**, 033835, (2008); J. F. Zhang, Q. Tian, Y. Y. Wang, C. Q. Dai, and L. Wu, *ibid.* **81**, 023832 (2010); C. Q. Dai, Y. Y. Wang, and C. J. Yan, Opt. Commun. **283**, 1489 (2010).

[15] X. Y. Tang and P. K. Shukla, Phys. Rev. A **76**, 013612 (2007).

[16] H. Michinel, José R. Salgueiro, and María J. Paz-Alonso, Phys. Rev. E **70**, 066605 (2004); María J. Paz-Alonso and H. Michinel, Phys. Rev. Lett. **94**, 093901 (2005).

[17] A. Vinçotte and L. Bergé, Phys. Rev. Lett. **95**, 193901 (2005); Phys. Rev. A **70**, 061802 (2004); Physica D **223**, 163 (2006); S. Champeaux, L. Bergé, D. Gordon, A. Ting, J. Peñano, and P. Sprangle, Phys. Rev. E **77**, 036406 (2008).

[18] A. Hasegawa and E. Tappert, Appl. Phys. Lett. **23**, 142 (1973); Govind P. Agrawal, *Nonlinear Fiber Optics* (Academic, San Diego, CA, 1995).

[19] K. Staliunas, O. Egorov, Y. S. Kivshar, and F. Lederer, Phys. Rev. Lett. **101**, 153903 (2008); O. A. Egorov, F. Lederer, and K. Staliunas, Phys. Rev. A **82**, 043830 (2010).

[20] F. Dalfovo, S. Giorgini, L. P. Pitaevskii, and S. Stringari, Rev. Mod. Phys. **71**, 463 (1999).

[21] K. Staliunas, S. Longhi, and G. J. deValcarcel, Phys. Rev. Lett. **89**, 210406 (2002); H. Saito and M. Ueda, *ibid.* **90**, 040403 (2003); F. Kh. Abdullaev, J. G. Caputo, R. A. Kraenkel, and B. A. Malomed, Phys. Rev. A **67**, 013605 (2003).

[22] A. T. Avelar, D. Bazeia, and W. B. Cardoso, Phys. Rev. E **79**, 025602(R) (2009).

[23] W. B. Cardoso, A. T. Avelar, and D. Bazeia, Phys. Lett. A **374**, 2640 (2010).

[24] W. B. Cardoso, A. T. Avelar, D. Bazeia, and M. S. Hussein, Phys. Lett. A **374**, 2356 (2010); J. Belmonte-Beitia and G. F. Calvo, *ibid.* **373**, 448 (2009).

[25] J. Belmonte-Beitia, V. M. Pérez-García, V. Vekslerchik, and P. J. Torres, Phys. Rev. Lett. **98**, 064102 (2007); J. Belmonte-Beitia, V. M. Perez-Garcia, V. Vekslerchik, and V. V. Konotop, *ibid.* **100**, 164102 (2008).

[26] X. G. He, D. Zhao, L. Li, and H. G. Luo, Phys. Rev. E **79**, 056610 (2009).

[27] F. Kh. Abdullaev, A. M. Kamchatnov, V. V. Konotop, and V. A. Brazhnyi, Phys. Rev. Lett. **90**, 230402 (2003).

[28] W. P. Zhong, M. Belić, Y. Q. Lu, and T. W. Huang, Phys. Rev. E **81**, 016605 (2010).

[29] J. C. Bronski, L. D. Carr, B. Deconinck, and J. N. Kutz, Phys. Rev. Lett. **86**, 1402 (2001); J. C. Bronski, L. D. Carr, R. Carretero-González, B. Deconinck, J. N. Kutz, and K. Promislow, Phys. Rev. E **64**, 056615 (2001); J. C. Bronski, L. D. Carr, B. Deconinck, J. N. Kutz, and K. Promislow, *ibid.* **63**, 036612 (2001); G. Theocharis, D. J. Frantzeskakis, R. Carretero-González, P. G. Kevrekidis, and B. A. Malomed,

ibid. **71**, 017602 (2005); A. Gubeskys and B. A. Malomed, Phys. Rev. A **75**, 063602 (2007); S. Walter, D. Schneble, and A. C. Durst, *ibid.* **81**, 033623 (2010).

[30] V. N. Serkin, V. M. Chapela, J. Percino, and T. L. Belyaeva, Opt. Commun. **192**, 237 (2001); G. Yang, R. Hao, L. Li, Z. Li, and G. Zhou, *ibid.* **260**, 282 (2006); J. Wang, L. Li, and S. Jia, J. Opt. Soc. Am. B **25**, 1254 (2008); W. P. Zhong and M. R. Belić, Phys. Rev. E **81**, 056604 (2010).

[31] Kh. I. Pushkarov *et al.*, Opt. Quantum Electron. **11**, 471 (1979); Kh. I. Pushkarov and D. I. Pushkarov, Rep. Math. Phys. **17**, 37 (1980); D. I. Pushkarov and S. Tanev, Opt. Commun. **124**, 354 (1996); S. Tanev and D. I. Pushkarov, *ibid.* **141**, 322 (1997); Pavel Honzatko, *ibid.* **127**, 363 (1996); N. Akhmediev and A. Ankiewicz, *Solitons: Nonlinear Pulses and Beams* (Chapman & Hall, London, 1997); R. Y. Hao, L. Li, Z. H. Li, R. C. Yang, and G. S. Zhou, *ibid.* **245**, 383 (2005).

[32] D. E. Pelinovsky, V. V. Afanasjev, and Y. S. Kivshar, Phys. Rev. E **53**, 1940 (1996).

[33] F. Kh. Abdullaev, A. Gammal, L. Tomio, and T. Frederico, Phys. Rev. A **63**, 043604 (2001).

[34] T. S. Raju and P. K. Panigrahi, Phys. Rev. A **81**, 043820 (2010); J. F. Wang, L. Li, and S. T. Jia, J. Opt. Soc. Am. B **25**, 1254 (2008).

[35] L. P. Pitaevskii and S. Stringari, *Bose-Einstein Condensation* (Oxford University Press, Oxford, 2003); H. Pu, L. O. Baksmaty, W. Zhang, N. P. Bigelow, and P. Meystre, Phys. Rev. A **67**, 043605 (2003); B. Eiermann, P. Treutlein, Th. Anker, M. Albiez, M. Taglieber, K.-P. Marzlin, and M. K. Oberthaler, Phys. Rev. Lett. **91**, 060402 (2003); S. K. Adhikari, Phys. Rev. E **71**, 016611 (2005); F. Kh. Abdullaev, B. B. Baizakov, and M. Salerno, *ibid.* **68**, 066605 (2003); H. Sakaguchi and B. A. Malomed, J. Phys. B **37**, 1443 (2004).

[36] W. P. Zhong, M. Belić, Y. Q. Lu, and T. W. Huang, Phys. Rev. E **81**, 016605 (2010).

[37] S. Peil, J. V. Porto, B. Laburthe Tolra, J. M. Obrecht, B. E. King, M. Subbotin, S. L. Rolston, and W. D. Phillips, Phys. Rev. A **67**, 051603(R) (2003); Q. Q. Zhu, W. H. Hai, and S. G. Rong, Phys. Rev. E **80**, 016203 (2009); P. J. Y. Louis, E. A. Ostrovskaya, and Y. S. Kivshar, Phys. Rev. A **71**, 023612 (2005).

[38] Y. S. Kivshar and B. A. Malomed, Rev. Mod. Phys. **61**, 763 (1989).

[39] R. Atre, P. K. Panigrahi, and G. S. Agarwal, Phys. Rev. E **73**, 056611 (2006); S. Kumar and A. Hasegawa, Opt. Lett. **22**, 372 (1997); V. N. Serkin and A. Hasegawa, Phys. Rev. Lett. **85**, 4502 (2000).

[40] See, e.g., I. Bloch, Nat. Phys. **1**, 23 (2005); A. D. Cronin *et al.*, Rev. Mod. Phys. **81**, 1051 (2009); M. Nest, Y. Japha, R. Folman, and R. Kosloff, Phys. Rev. A **81**, 043632 (2010).

[41] D. Poletti, T. J. Alexander, E. A. Ostrovskaya, B. W. Li, and Y. S. Kivshar, Phys. Rev. Lett. **101**, 150403 (2008).

[42] C. F. Bharucha, K. W. Madison, P. R. Morrow, S. R. Wilkinson, B. Sundaram, and M. G. Raizen, Phys. Rev. A **55**, R857 (1997); G. Ritt, C. Geckeler, T. Salger, G. Cennini, and M. Weitz, *ibid.* **74**, 063622 (2006); A. S. Mellish, G. Duffy, C. McKenzie, R. Geursen, and A. C. Wilson, *ibid.* **68**, 051601(R) (2003).

[43] T. Mayteevarunyoo and B. A. Malomed, Phys. Rev. A **74**, 033616 (2006).

[44] T. Salger, C. Geckeler, S. Kling, and M. Weitz, Phys. Rev. Lett. **99**, 190405 (2007); Z. Y. Yang, L. C. Zhao, T. Zhang, Y. H. Li, and R. H. Yue, Phys. Rev. A **81**, 043826 (2010).

[45] K. T. Stoychev, M. T. Primatarowa, and R. S. Kamburova, Phys. Rev. E **73**, 066611 (2006); **70**, 066622 (2004); M. T. Primatarowa, K. T. Stoychev, and R. S. Kamburova, *ibid.* **72**, 036608 (2005).

[46] J. F. Zhang, Y. S. Li, J. P. Meng, L. Wu, and B. A. Malomed, Phys. Rev. A **82**, 033614 (2010).